ELSEVIER

Journal of Organometallic Chemistry 539 (1997) 27–35

Journal of Organometallic Chemistry

Syntheses and characterization of $OsPt_2(\mu\text{-}CO)(\mu\text{-}I)_2(CO)_2(PPh_3)_3$ and $Os_2(\mu\text{-}I)_2(CO)_{6-n}(PPh_3)_n$ $(n = 1, 2)$ in the solid-state and solution [1]

V.A. Maksakov *, V.P. Kirin, A.V. Virovets, S.V. Tkachev, V.I. Alekseev, N.V. Podberezskaya

Institute of Inorganic Chemistry, Siberian Division of RAS, Acad. Lavrentyev str. 3, Novosibirsk 630090, Russia

Received 24 June 1996; accepted 26 November 1996

Abstract

The reaction of $Os_2(CO)_6(\mu\text{-}I)_2$ with $Pt(dba)(PPh_3)_2$ or $Pt(PhCCPh)(PPh_3)_2$ affords three novel complexes $Os_2(CO)_{6-n}(\mu\text{-}I)_2(PPh_3)_n$ [$n = 1$ (**2**), $n = 2$ (**4**)] and $OsPt_2(CO)_2(\mu\text{-}CO)(\mu\text{-}I)_2(PPh_3)_3$ (**3**). **2** and **3** were characterized by X-ray analysis. The isotopically pure $^{187}Os_2(CO)_6(\mu\text{-}I)_2$ was also used in the synthesis of the corresponding complexes **2′–4′** to study their structures in solution. It was determined that the $OsPt_2(CO)_2(\mu\text{-}CO)(\mu\text{-}I)_2(PPh_3)_3$ cluster is symmetric in solution whereas in the solid-state it has an asymmetric structure which may be explained by the different disposition of the μ-I ligands around the $OsPt_2$-triangle. ^1J(Os–Os), ^2J(Os–P), ^1J(Pt–Pt), ^1J(Pt–P), and ^2J(P–P) coupling constants have been determined. © 1997 Elsevier Science S.A.

Keywords: Osmium; Platinum; Carbonyl clusters; Solid-state structure; Solution structure

1. Introduction

One of the most logical strategies for the synthesis of heterometal cluster complexes is to build them using low-nuclear fragments, for example by the addition reaction of a coordinatively unsaturated metal fragment across a metal–metal bond or the substitution reaction of anionic ligands by a carbonyl metalate anion [1]. These methods have been successfully used by us in the synthesis of the iron–osmium clusters $Os_2Fe(CO)_{10}(\mu\text{-}X)_2$ (X = OH, I) starting from binuclear carbonyl osmium halides [2].

The present paper is devoted to the synthesis and structural study of the homo- and heteronuclear complexes $Os_2(CO)_{6-n}(\mu\text{-}I)_2(PPh_3)_n$ [$n = 1$ (**2**), $n = 2$ (**4**)] and $OsPt_2(CO)_2(\mu\text{-}CO)(\mu\text{-}I)_2(PPh_3)_3$ (**3**), resulting from the reaction of $Os_2(CO)_6(\mu\text{-}I)_2$ with $Pt(dba)(PPh_3)_2$ (dba = dibenzelidenacetone) or $Pt(PhCCPh)(PPh_3)_2$. The isotopically pure $^{187}Os_2(CO)_6(\mu\text{-}I)_2$ was used as the starting complex as well as the compound with a natural isotope content. The presence of several magnetically active nuclei (^{31}P, ^{187}Os, ^{195}Pt) in the compounds makes NMR an effective method for studying their structures in solution. Furthermore, when introducing the magnetically active ^{187}Os isotope into the complexes, we hoped to obtain novel data on ^{187}Os NMR, in particular to determine $^1J(^{187}Os–^{187}Os)$, $^1J(^{187}Os–Pt)$, $^2J(^{187}Os–P)$, and $^2J(^{187}Os–P)$ coupling constants.

2. Results and discussion

The mononuclear complexes $Pt(dba)(PPh_3)_2$ and $Pt(PhCCPh)(PPh_3)_2$ were used for the synthesis of a platinum–osmium heterometal cluster using $Os_2(CO)_6(\mu\text{-}I)_2$ as the starting building block. The analogous $Pt(alkene)(PPh_3)_2$ complexes have been used extensively in the synthesis of heterometallic platinum-containing clusters [3].

The interaction of $Os_2(CO)_6(\mu\text{-}I)_2$ (**1**) with one equivalent of $Pt(dba)(PPh_3)_2$), obtained in situ at room temperature, results in a single compound, which decomposes during chromatography on silica. At 80 °C,

* Corresponding author.

[1] Dedicated to the memory of Yu.T. Struchkov.

PII S0022-328X(96)06959-8

this reaction affords two novel complexes which may be separated by chromatography:

$$Pt(dba)_2 \xrightarrow[\text{benzene}]{2PPh_3,\ 20\,^\circ C} Pt(dba)(PPh_3)_2 \xrightarrow[\text{benzene}]{Os_2(CO)_6I,\ 80\,^\circ C}$$

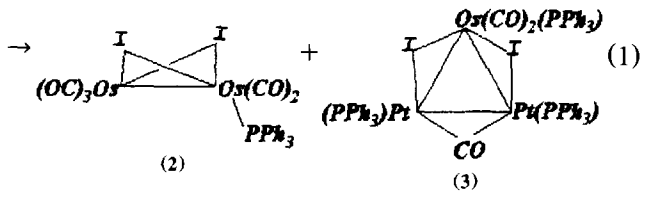

(1)

The mass spectrum of the main product displays the parent ion at m/z 1040 (on ^{192}Os) with a subsequent loss of five CO ligands, corresponding to $Os_2(CO)_5(PPh_3)(\mu\text{-}I)_2$ (**2**). IR and $^{31}P\{^1H\}$ spectral data (see Section 3 and Table 1) correlate well with this formulation. The structure of this complex was solved conclusively by X-ray analysis (Fig. 1).

The crystal structure of $Os_2(CO)_6(\mu\text{-}I)_2$ (**1**) was previously described in Ref. [4]. Compound **2** is a product of the substitution of the carbonyl group disposed along the Os–Os vector in **1** by the PPh_3 ligand. The geometrical characteristics of **1** and **2** such as Os–Os, Os–I, Os–C bond lengths, and angles between Os_2I planes, differ insignificantly.

Apart from stretching bands about 2000 cm^{-1}, the IR spectrum of **3** displays a CO stretching band at 1766 cm^{-1} implying the presence of at least one bridging or semibridging CO group. It is impossible to obtain more detailed information on the complex from IR spectra. Also, the mass spectrum of this compound, in contrast to that of **2**, does not contain the expected parent ion. Because of this, the main structural information was obtained from the X-ray analysis.

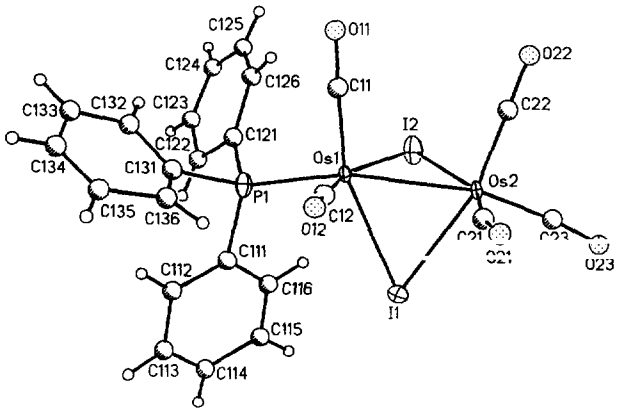

Fig. 1. Molecule $Os_2(\mu\text{-}I)_2(CO)_5(PPh_3)$ (**2**) (50% probability thermal ellipsoids when possible).

The molecular structure of **3** is shown in Fig. 2. Only a few cluster compounds with $OsPt_2$ and $RuPt_2$ cores have been structurally characterized previously: $MPt_2(\mu\text{-}CO)_3(PPh_3)_3(CO)_2$ (M = Os, **5a** [5]; M = Ru, **5b**, [6]), $RuPt_2(\mu\text{-}CO)_3(PMePh_2)_3(CO)_2$ (**6** [7]) and $OsPt_2(\mu,\eta^2\text{-}CH_3CCCH_3)(PPh_3)_2(CO)_5$ (**7** [8]). All these, except for the latter, contain the $Pt(\mu\text{-}CO)Pt$ fragment. The molecular structures of **5a** and **6** seem to be similar to that of **3**. But there is a difference in their electronic structures. In **5** and **6** every μ-CO ligand at the Os–Pt bond donates two cluster valence electrons (CVE) to the cluster core [9], whereas in **3**, μ-I ligands donate three CVE each. Therefore **3** has a different

Table 1
$^{31}P\{^1H\}$ and $^{195}Pt\{^1H\}$ NMR spectra of $Os_2(CO)_5(PPh_3)(\mu\text{-}I)_2$ (**2**), $Os_2(CO)_4(PPh_3)_2(\mu\text{-}I)_2$ (**4**), and $Pt_2Os(CO)_2(\mu\text{-}CO)(PPh_3)_3(\mu\text{-}I)_2$ (**3**) and their ^{187}Os-labeled analogues in $CDCl_3$

Compound	δ(P) [a]	δ(Pt) [b]	Coupling constants (Hz)
2(2′)	8.6		^1J(Os–P) = 218.9 ^2J(Os–P) = 12.6
4(4′)	8.6		^1J(Os–Os) = 21.7 or 5.4, ^2J(Os–P) = 5.7 [c], ^3J(P–P) = 5.4 or 21.7, ^1J(Os–P) = 217.4 [c]
3(3′)	3.9 [P(3)] 42.8 [P(1,2)]	−4396	^1J(Pt–P) = 5728 ^2J(Pt–P) = 615 [P(1), P(2)] [d] ^2J(Pt–P) = 34 [P(3)] ^1J(Os–P) = 219 [P(3)] ^2J(Os–P) = 13 [P(1), P(2)] ^3J(P–P) = 35 ^1J(Pt–Pt) = 3550 ± 50

[a] Relative to 85% H_3PO_4.
[b] Relative to 2M H_2PtCl_6 solution in 2M HCl.
[c] The signs of ^1J(Os,P) and ^2J(Os,P) are opposite.
[d] ^2J(Pt,P(1)), ^2J(Pt,P(2)) > 0

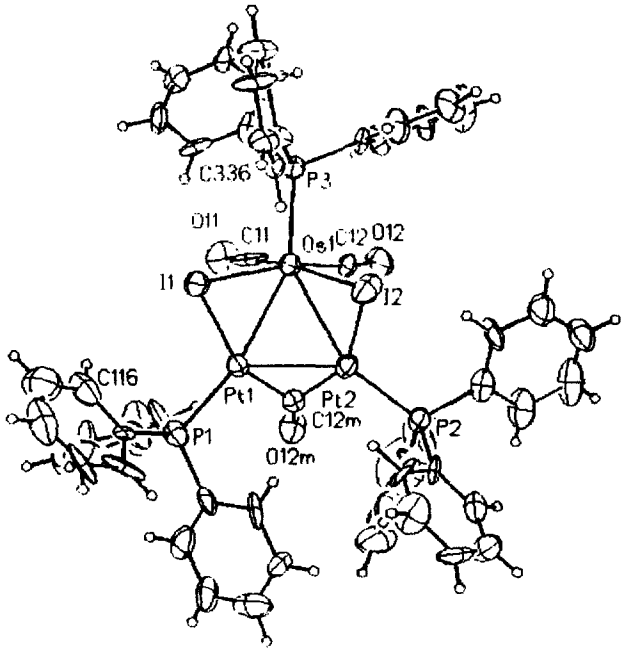

Fig. 2. Molecule $OsPt_2(\mu\text{-}CO)(\mu\text{-}I)_2(CO)_2(PPh_3)_3$ (**3**) in projection on $OSPt_2$ plane (40% probability thermal ellipsoids).

Table 2
Bond distances for $3 \cdot \frac{1}{2}C_6H_{14}$

Atoms	Bond length (Å)	Atoms	Bond length (Å)
Os(1)–Pt(1)	2.796(2)	Os(1)–C(11)	1.75(4)
Os(1)–Pt(2)	2.852(2)	Os(1)–C(12)	1.87(3)
Pt(1)–Pt(2)	2.685(2)	Pt(1)–C(12M)	1.97(3)
Os(1)–I(1)	2.769(2)	Pt(2)–C(12M)	1.94(3)
Os(1)–I(2)	2.787(2)	C(11)–O(11)	1.24(3)
Pt(1)–I(1)	2.694(2)	C(12)–O(12)	1.13(3)
Pt(2)–I(2)	2.745(2)	C(12M)–O(12M)	1.17(3)
Os(1)–P(3)	2.380(8)	C(1S)–C(2S)	1.38(7)
Pt(1)–P(1)	2.248(8)	C(2S)–C(3S)	1.50(11)
Pt(2)–P(2)	2.250(8)	C(3S)–C(3S) [a]	1.07(13)

[a] Atom is transformed by symmetry operation $1-x, 1-y, -z$.

number of CVE to **5a** and **6**: 46 (18 from ligands, **8** from Os and 2×10 from Pt) and 44 (16 from ligands, 8 from Os and 2×10 from Pt) respectively. All these clusters are electron-deficient compounds since a triangle metal core must have $N = 48$ according to the effective atomic number (EAN) rule [10].

The different electronic structures of **3** and **5a** and **6** mentioned above cause differences in the ligand coordination sphere: in **5a** and **6** the PPh_3 ligand at the Os atom occupies an axial position with respect to the $OsPt_3$ plane and all μ-CO lie practically in this plane; however, in **3**, all PPh_3 ligands are in the equatorial position and both μ-I lie in the semiaxial and axial positions.

The most interesting feature of complex **3** is that the μ-I ligands are coordinated asymmetrically: the angles between the $OsPt_2$ and OsPtI planes are 42° and 85° for I(1) and I(2) respectively; the bond lengths in Os(1)Pt(1)I(1) and Os(1)Pt(2)I(2) triangles are also different (Table 2). Compounds **5a,b** and **6** are more symmetrical when compared with **3**: the difference between the two Os–Pt bond lengths are 0.056(2) Å, 0.009(1) Å, 0.007(1) Å and 0.022(2) Å for **3**, **5a,b** and **6** respectively. A possible reason for this is, in our opinion, the disposition of the PPh_3 ligands. These ligands at Pt(1) and Pt(2) lie asymmetrically with respect to the line between the Os atom and the center of the Pt–Pt bond (Fig. 2). They have a different conformation: the angles between the phenyl ring planes are 88.6, 64.6, 95.0° and 108.7, 62.8, 109.5° for P(1)Ph_3 and P(2)Ph_3 respectively. A possible reason for this is the steric hinderance between the bulky μ-I and PPh_3 groups in the same molecule along with the intermolecular C(Ph) · · · C(Ph) contacts of 3.40–3.50 Å. It should be taken into account that the equatorial coordination of the PPh_3 ligand at the Os atom may also cause a steric 'pushing' of the μ-I ligands out of $OsPt_2$ plane. In the molecular structure of **3** there are some C(Ph) · · · I contacts shorter than the sum of van der Waals radii (3.8 Å [11]): I(1) · · · C(116) of 3.664 and I(2) · · · C(336) of 3.738 Å. In brief, we conclude that the asymmetrical turning of the PPh_3 ligands through the intramolecular interactions results in the asymmetrical coordination of the iodine atoms. The latter may be a reason for differences in the Os–Pt, Os–I and Pt–I bond lengths. As for compounds **5a** and **6**, they have the equatorial μ-CO ligands symmetrically coordinated to both Os–Pt bonds in agreement with the larger symmetry of the $OsPt_2$ triangle.

A possible reason for the formation of the large amount of **2** in high yield during the reaction might be the facile substitution of CO by PPh_3, which is present in a free state in the solution due to the preparation of $Pt(dba)(PPh_3)_2$ in situ from $Pt(dba)_2$ and PPh_3. To avoid this, the reaction of $Os_2(CO)_6(\mu\text{-}I)_2$ was conducted using $Pt(PhCCPh)(PPh_3)_2$. However, this reaction again results in a large amount of **2** together with **3** and one new product whose IR spectrum contains stretching bands of terminal CO groups only. The mass spectrum of this product displays the parent ion at m/z 1274 (on ^{192}Os) with the subsequent loss of four CO ligands, corresponding to $Os_2(CO)_4(\mu\text{-}I)_2(PPh_3)_2$ (**4**). The $^{31}P\{^1H\}$ spectrum reveals a singlet whose chemical shift (8.63 ppm) almost coincides with that of **2**. This fact proposes that the phosphine ligands coordinate to different osmium atoms:

$$Pt(PhCCPh)(PPh_3)_2 \xrightarrow[\text{benzene}]{Os_2(CO)_6I_2,\ 80\,^\circ C} \rightarrow \text{(2)} + \text{(3)} \quad (2)$$

L = CO (2)
PPh_3 (4)

The analysis of reactions **1** and **2** permits the suggestion that complex **2** is not the product of the direct substitution of CO by PPh_3 in $Os_2(CO)_6(\mu\text{-}I)_2$. The product is more likely to be that of the decomposition of an intermediate '$Os_2Pt(CO)_6(PPh_3)_2(\mu\text{-}I)_2$' forming in the first step of the interaction of $Os_2(CO)_6(\mu\text{-}I)_2$ with $Pt(dba)(PPh_3)_2$ or $Pt(PhCCPh)(PPh_3)_2$.

^{187}Os-labeled analogues (**2'**–**4'**) of complexes **2**–**4** were obtained starting from $^{187}Os_2(CO)_6(\mu\text{-}I)_2$ for a more effective study of their structures in solution by NMR techniques.

The chemical shifts of the phosphorus atoms in clusters **2**, **4**, **2'**, and **4'** are essentially the same within experimental error (δ 8.6 ppm). $^{31}P\{^1H\}$ spectra of **2** and **4** are singlets. The small downfield shift of the PPh_3 ligand resonance with respect to that of free triphenylphosphine [12] ($\Delta\delta$ 15.1 ppm) is consistent with the coordination of PPh_3 to the osmium atom [8,13].

The $^{31}P\{^1H\}$ spectra of **2'** and **4'** are more informative and allow a determination of the nuclearities of the compounds. Thus, the $^{31}P\{^1H\}$ spectrum of **2'** is a doublet of doublets, corresponding to the ASX (A ≡ P) spin system due to the presence of the P–Os–Os unit in the molecule. The measured values of ^1J(Os–P) and ^2J(Os–P) are given in Table 1. The magnitude of ^1J(Os–P) (218.9 Hz) is close to coupling-constants previously determined in the complexes $OsH_4(PEt_2Ph)_3$ and *cis*-$OsCl_2(CO)_2(PBuPr_2)_2$ (166 Hz and 149.3 Hz respectively) [14].

According to the classification proposed by Bernstein, Pople and Schneider [15] the $^{31}P\{^1H\}$ spectrum of **4'** is ascribed as that of a AA'XX' spin system due to the presence of the P–Os–Os–P unit containing four magnetically non-equivalent nuclei. The spectra of this type are characterized by the identical A- and X-subspectra containing ten separate peaks. The analysis of the distances between peaks of the outer and inner quartets in the $^{31}P\{^1H\}$ spectrum of **4'** makes it possible to determine four auxiliary parameters: $L = {}^1J(POs) - {}^2J(POs)$, $K = {}^1J(OsOs) + {}^3J(PP)$, $M = {}^1J(OsOs) - {}^3J(PP)$, $N = {}^1J(POs) + {}^2J(POs)$. Based on these it is possible to calculate all four characterizing spectrum coupling constant analyses of the second-order spectrum by a common method [15]. It is appeared that the ^1J(Os–P) and ^2J(Os–P) coupling constants (Table 1) to be opposite in sign. The ^1J(Os–P) value in **4'** was chosen by coincidence with that of ^1J(Os–P) in **2'**. The remaining two coupling constants ^1J(Os–Os) and ^3J(P–P) are assigned as 21.7 Hz and 5.4 Hz respectively. However, in this case it is impossible to make an unambiguous assignment of the coupling constant values. The validity of the analysis is confirmed by the close correspondence of the experimental spectrum to that simulated on the basis of the measured parameters (Fig. 3).

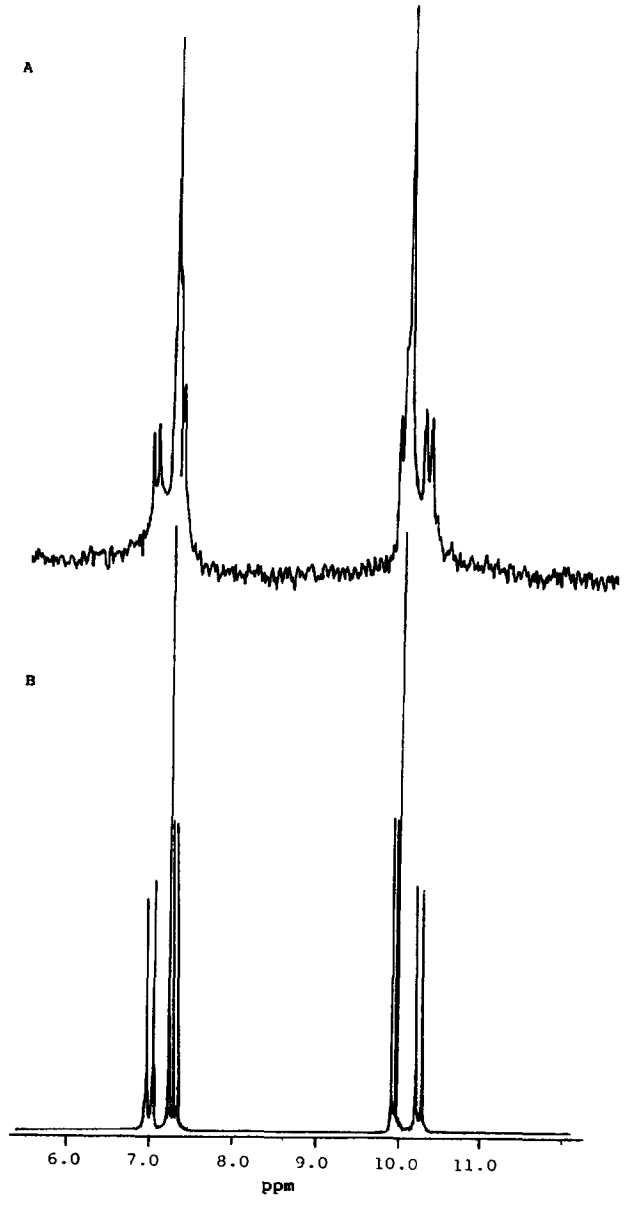

Fig. 3. Experimental ($CDCl_3$, room temperature) (A) and simulated (B) $^{31}P\{^1H\}$ NMR spectra of **4'**.

The method of analysis of the platinum compound spectra is based on the fact that the real spectrum is a superposition of the spectra corresponding to isotopomers arising from the statistical distribution of Pt in the different sites in the molecule. For molecule **3**, with two platinum atoms, the isotopomer content is as follows: 44% of molecules contain no ^{195}Pt nuclei (**3a**), in 44.6% one of the atoms is a ^{195}Pt nucleus (**3b**), and in 11.4% both atoms are ^{195}Pt nuclei (**3c**).

For convenience, let the platinum and phosphorus atoms in cluster **3** (CO, I ligands and Ph groups are omitted for clarity) be numbered as follows:

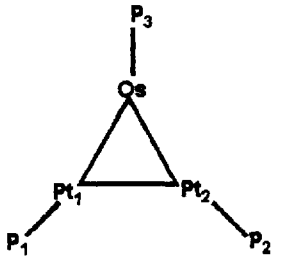

It is apparent from the spectrum of **3** (Fig. 4) that the molecule contains two types of PPh_3 (δ 3.9 and 42.8 ppm) in a 1:2 ratio. The multiplet with δ = 3.9 can be assigned to the PPh_3 group coordinated on the osmium atom [P(3)], and the second multiplet corresponds to the triphenylphosphine groups coordinated to the platinum atoms (P(1) and P(2)). For phosphine groups coordinated to platinum atoms the resonances of the PPh_3 phosphorus atom are generally shifted downfield 25–70 ppm relative to the free ligand [8,16–21].

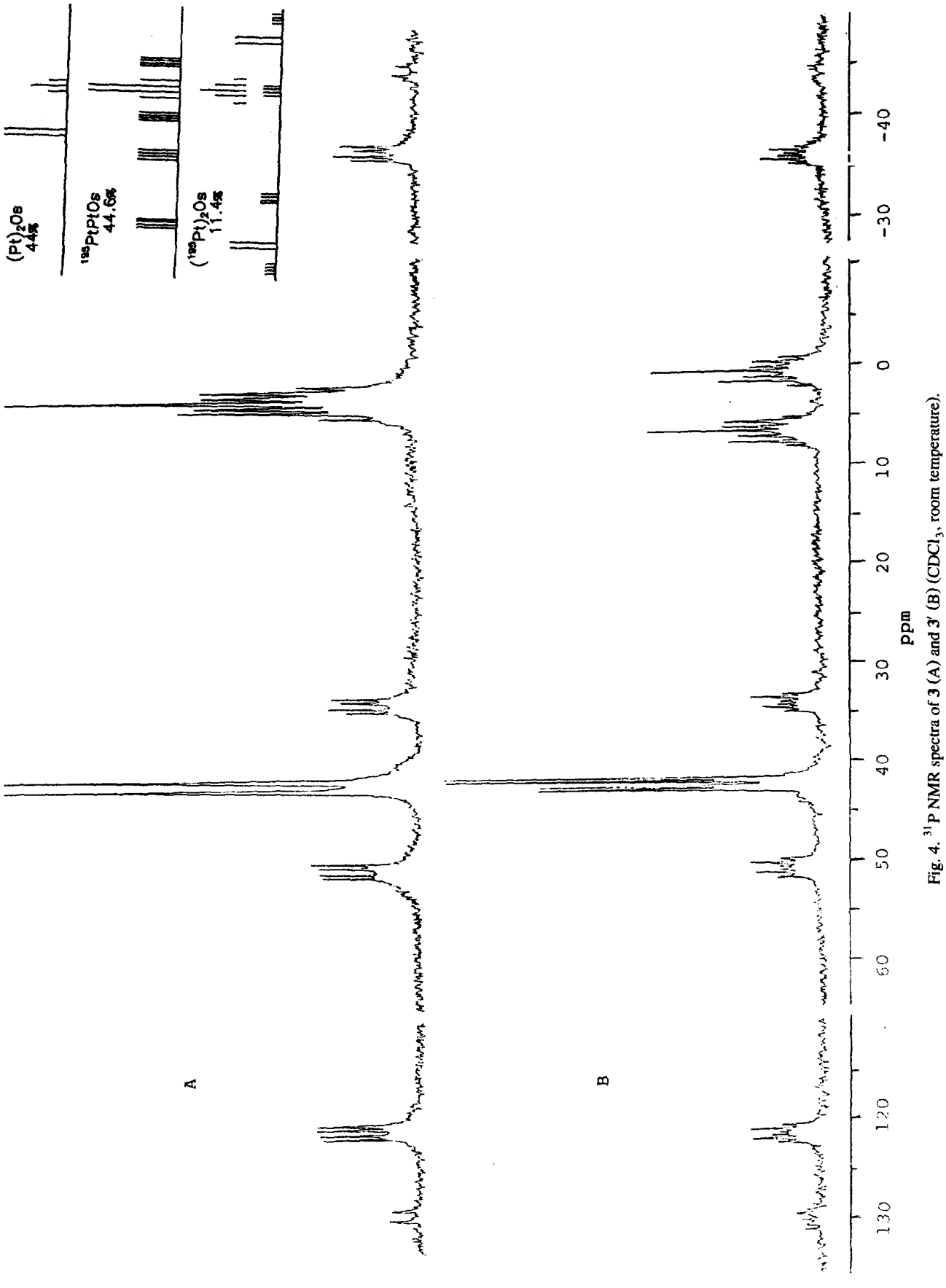

Fig. 4. ^{31}P NMR spectra of **3** (*A*) and **3'** (*B*) ($CDCl_3$, room temperature).

The doublet splitting of the most intense resonance, corresponding to the P(1) and P(2) nuclei of isotopomer **3a** allows the immediate determination of ^{3}J(P(1,2)–P(3)) = 35 Hz. The significant difference in the P(1) and P(2) chemical shift relative to that of P(3) makes it possible to interpret the spin systems of **3a**, **3b** and **3c** as AM, AA′MX, and AA′MXX′ (X ≡ Pt) respectively. Thus, the subspectra of the P(1)–Pt(1)–Pt(2)–P(2) unit of isotopomers **3b** and **3c** are reduced to spectra of the AA′X and AA′XX′ types in which each component is further split to a doublet on the P(3) spin. The pseudo first-order of the $^{31}P\{^{1}H\}$ and $^{195}Pt\{^{1}H\}$ spectra for isotopomer **3b** caused by the high magnitude of ^{1}J(Pt–P) [22] permits the determination of all coupling constants except that of ^{1}J(PtPt). The value of the latter and the relative signs of ^{1}J(Pt–P) and ^{2}J(Pt–P) were established from $^{195}Pt\{^{1}H\}$ spectra of isotopomer **3c** (Table 1).

All components in the $^{31}P\{^{1}H\}$ spectrum of cluster **3′** are further split to doublets by the ^{187}Os nucleus spin. The measured values of the ^{187}Os–^{3}P coupling constants are given in Table 1. Unfortunately, the ^{1}J(Pt–Os) coupling constant failed to be established owing to the low resolution of the $^{195}Pt\{^{1}H\}$ spectrum (see Section 3). However, it is apparent that its magnitude does not exceed 10 Hz. The small value of ^{1}J(Pt–Os) might be caused by a strong trans-influence of the triphenylphosphine groups which are coordinated on Pt in **3** practically trans to the PtOs bonds (PPtOs angles are 154 and 164°). The validity of the analysis is confirmed by a good agreement between the experimental and calculated spectra.

The data in Table 1 deserve further comment. The chemical shift of Pt in cluster **3** falls into the region which is characteristic of a formal charge on the platinum atom of (0) [13]. According to X-ray analysis data for **3**, Pt(1) and Pt(2) as well as P(1) and P(2) atoms have a different symmetry in the solid-state. The equivalence of the chemical shifts and coupling constants from the NMR spectra is indicative of the identical environments of the corresponding phosphorus and platinum atoms in solution. We propose that the cluster symmetry in solution is effectively increased by rapid dynamic processes such as intramolecular vibrations or an exchange of the ligands. A stereochemical non-rigidity of metal carbonyl clusters is observed quite often [23,24].

A correlation between a ^{1}J(PtP) magnitude and the Pt–P bond distance has been previously reported in phosphine Pt(IV) and Pt(II) complexes [25] and in dimeric Pt(I) complexes with a bridging ddpm ligand [26]. We have decided to reveal the presence of such a correlation for complexes in which platinum has a zero formal oxidation state. Numerous data on the ^{1}J(PtP) constants, mostly concerning cluster Pt(0) complexes [17,18,22,27–32], provide this. The results are given in

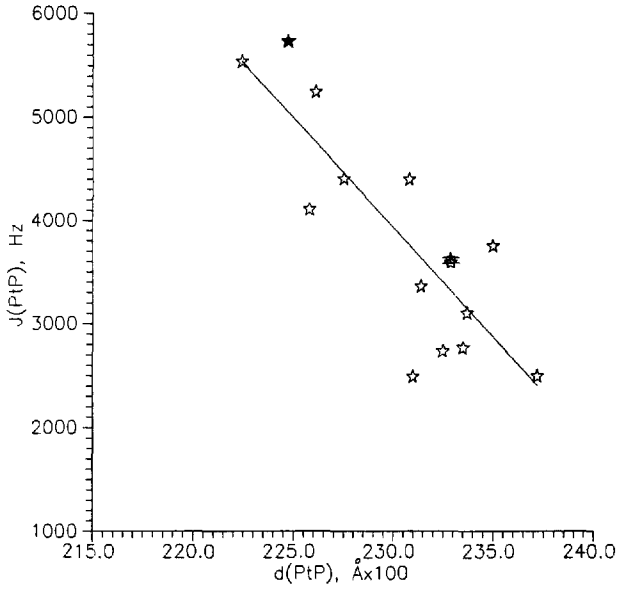

Fig. 5. Correlation of ^{1}J(Pt–P) values with Pt–P bond distances for Pt(0) cluster compounds. Dotted sign denotes $OsPt_2(\mu\text{-}CO)(\mu\text{-}I)_2(CO)_2(PPh_3)_3$ (this work).

Fig. 5. In spite of the significant point spread of the plot, caused by a high sensitivity of the coupling constants to a relative disposition of substituents around phosphorus and platinum atoms, it is apparent that the correlation between ^{1}J(PtP) and the metal–phosphine bond length is also present in the case of Pt(0).

The chemical shift value and the relationship of the ^{1}J(Pt–P) and ^{2}J(PtP) values found for **3** allow the platinum atoms to be assigned by the formal '0' charge in this cluster.

3. Experimental section

3.1. General procedures

The reactions were carried out under an argon atmosphere using freshly distilled solvents. The starting compounds, $Os_2(CO)_6(\mu\text{-}I)_2$ [33], $Pt(dba)_2$ [34], and $Pt(PPh_3)_2(PhCCPh)$ [35] were prepared by the previously described procedures. The reaction course was monitored by thin layer chromatography (TLC) on Silufol plates. The preparative chromatography was performed on a silica (μ 40/100) column.

IR spectra were obtained on a Specord IR-75 spectrophotometer, the electron impact mass spectra were obtained on a MX-310 mass spectrometer at an ionizing voltage of 70 eV.

Approximately 0.02 $M l^{-1}$ solutions of the cluster complexes in $CDCl_3$ were used to obtain NMR spectra. $^{31}P\{^{1}H\}$ and $^{195}Pt\{^{1}H\}$ spectra were recorded on a Bruker SXP-4-100 spectrometer (36.46 MHz and 19.29 MHz respectively) with the sample spinning and the field

stabilization on the signal of the solvent deuterium. ^{195}Pt spectra were also recorded on a Bruker CXP-300 (64.22 MHz). In this case the sample tube was orientated perpendicular to the solenoid axis to avoid the sensitivity loss caused by the use of the saddle coil. As a result, the resolution in the spectrum was ca. 10 Hz due to an impossibility of the sample spinning. The chemical shifts (±0.5 ppm), positive downfield, have been recorded relative to the external standards (85% H_3PO_4 and 2 M H_2PtCl_6 solution in 2 N HCl for ^{31}P and ^{195}Pt respectively) and are given in Table 1. The coupling constants (±2 Hz) are given in the same table. All spectra were recorded at room temperature. The spectra simulation was made using the NMRCAL program which is available from the spectrometer producer.

3.2. The reaction of $Os_2(CO)_6(\mu\text{-}I)_2$ with $Pt(dba)_2$ and PPh_3

To 0.148 g (0.223 mmol) $Pt(dba)_2$ in 20 ml benzene, a solution of 0.120 g (0.458 mmol) PPh_3 in 15 ml benzene was added dropwise over a period of 1 h. After that, 0.181 g (0.225 mmol) $Os_2(CO)_6(\mu\text{-}I)_2$ was added to the resulting solution. TLC (hexane:benzene = 2:1.5) revealed that only one product was present in solution after 1 h stirring at room temperature. IR spectrum of the reaction mixture: (ν_{CO}, cm^{-1}) 2125w, 2112s, 2071s, 2049s, 2035sh, 2022vs, 2005sh, 1979m, 1949s, 1712w. The solution was refluxed for 2 h, evaporated to dryness and the solid residue chromatographed on a silica column (hexane:benzene = 2:1.75). The fractions were in order: yellow, $Os_2(CO)_6(\mu\text{-}I)_2$ (**1**) (6.5 mg); bright-yellow, $Os_2(CO)_5(\mu\text{-}I)_2(PPh_3)$ (103 mg, 66.4%) (**2**); red, $Pt_2Os(CO)_3(\mu\text{-}I)_2(PPh_3)_3$ (85 mg, 33.25%) (**3**). For $Os_2(CO)_5(\mu\text{-}I)_2(PPh_3)$ (**2**): IR spectrum (ν_{CO}, cm^{-1}, hexane): 2075s, 2012s, 1992s, 1949m. Mass spectrum displays the parent ion with m/z 1040 (^{192}Os). For $Pt_2Os(CO)_3(\mu\text{-}I)_2(PPh_3)_3$ (**3**): IR spectrum (ν_{CO}, cm^{-1}, CCl_4): 2005s, 1944m, 1766m.

Table 3
Crystallographic data of **2** and **3**·$\frac{1}{2}C_6H_{14}$

	2	**3**
Formula	$C_{23}H_{15}I_2O_5Os_3P$	$C_{60}H_{52}I_2O_3OsP_3Pt$
Molecular mass	1036.52	1748.11
Crystal system	monoclinic	monoclinic
a (Å)	25.14(2)	21.073(4)
b (Å)	12.243(7)	15.533(3)
c (Å)	18.70(1)	18.753(3)
β (deg)	114.32(5)	109.86(2)
Volume (Å^3)	5245(6)	5773(2)
ρ(calc) (g cm^{-3})	2.625	2.011
Space group, Z	$C2/c$, 8	$P2_1/c$, 4
Diffractometer	Syntex $P2_1$	CAD-4
Radiation	Cu Kα, λ = 1.5418 Å	Mo Kα, λ = 0.7107 Å
μ (cm^{-1})	373.50	82.25
Transmission (min, max)	0.248, 3.142	0.115, 0.850
Crystal size (mm^3)	0.25×0.20×0.13	0.25×0.20×0.018
Crystal color	orange	yellow-orange
Crystal shape	hexagonal plate	plate
2θ range (deg)	3–100	3–45
Reflections total /used	3705/2174 $F_o^2 > 0$	8210/3617 $F_o^2 > 2\sigma$
$R(F)$	0.0723 for obs.	0.0567 for obs.
$wR(F^2)$	0.1912 for all	0.1077 for all

Table 4
Atomic coordlnates (×10^4) and equivalent thermal parameters (Å^2 ×10^3) in **2**

Atom	x	y	z	$U_{iso/eq}$ [a]
Os(1)	2689(1)	601(1)	6557(1)	10(1)
Os(2)	3787(1)	206(1)	7650(1)	15(1)
I(1)	2975(1)	1029(2)	8125(1)	31(1)
I(2)	3013(1)	−1487(2)	7128(1)	26(1)
C(11)	2762(14)	252(24)	5656(17)	10(7)
O(11)	2830(12)	29(21)	5076(16)	48(8)
C(12)	2728(15)	1973(26)	6385(18)	16(8)
O(12)	2819(14)	2939(25)	6273(17)	65(9)
C(21)	3996(16)	1625(28)	7667(19)	24(9)
O(21)	4233(14)	2477(25)	7708(17)	62(9)
C(22)	4153(15)	−296(24)	7079(18)	14(8)
O(22)	4402(13)	−603(24)	6683(17)	62(9)
C(23)	4339(19)	−337(32)	8577(24)	42(11)
O(23)	4686(14)	−624(23)	9245(17)	59(8)
P(1)	1655(4)	435(7)	6030(5)	14(2)
C(111)	1320(13)	644(22)	6720(16)	4(7)
C(112)	881(14)	1398(24)	6554(18)	15(8)
C(113)	644(15)	1550(27)	7144(18)	24(9)
C(114)	835(19)	922(34)	7779(24)	52(12)
C(115)	1307(18)	179(31)	7944(23)	38(10)
C(116)	1521(16)	73(25)	7385(18)	19(8)
C(121)	1378(13)	−872(22)	5623(15)	4(7)
C(122)	848(16)	−1277(27)	5660(19)	24(9)
C(123)	636(18)	−2310(28)	5274(20)	31(10)
C(124)	884(16)	−2908(30)	4898(20)	28(9)
C(125)	1371(19)	−2449(33)	4862(23)	48(12)
C(126)	1601(19)	−1468(32)	5153(22)	45(11)
C(131)	1256(15)	1378(26)	5255(18)	18(8)
C(132)	876(15)	1006(28)	4539(19)	23(9)
C(133)	561(16)	1721(28)	3937(21)	28(9)
C(134)	664(20)	2841(36)	4097(26)	52(12)
C(135)	1039(17)	3225(31)	4746(21)	33(10)
C(136)	1410(20)	2448(31)	5358(24)	41(11)

[a] Defined as 1/3 of the trace of normalized U_{ij} tensor.

3.3. Reaction of $Os_2(CO)_6(\mu\text{-}I)_2$ with $Pt(PPh_3)_2(PhCCPh)$

0.067 g (0.084 mmol) $Os_2(CO)_6(\mu\text{-}I)_2$ and 0.0762 g (0.085 mmol) $Pt(PPh_3)_2(PhCCPh)$ in 10 ml benzene were stirred at room temperature for 30 min and then heated to reflux for 1 h. The solution was evaporated to dryness and the residue was chromatographed on silufol plates (hexane:benzene = 1:1) to afford bright-yellow, $Os_2(CO)_3(\mu\text{-}I)_2(PPh_3)$ (**2**) (49.4 mg, 57%); dark-yel-

Table 5
Atomic coordinates ($\times 10^4$) and equivalent thermal parameters (Å^2 $\times 10^3$) in $3 \cdot \frac{1}{2}C_6H_{14}$

Atom	x	y	z	U_{eq} [a]
Os(1)	7461(1)	−644(1)	1863(1)	37(1)
Pt(1)	8569(1)	458(1)	2427(1)	42(1)
Pt(2)	7352(1)	1088(1)	2311(1)	44(1)
I(1)	8679(1)	−1195(1)	2889(1)	54(1)
I(2)	6892(1)	−246(1)	2964(1)	60(1)
C(11)	7803(17)	−706(17)	1135(15)	61(10)
O(11)	8048(11)	−706(15)	619(12)	82(8)
C(12)	6731(15)	−71(18)	1166(19)	55(9)
O(12)	6285(11)	222(14)	706(12)	74(7)
C(12M)	8067(13)	1501(18)	1963(14)	41(7)
O(12M)	8165(10)	2078(13)	1614(11)	68(6)
C(1S)	5137(42)	4531(45)	−1343(49)	340(51)
C(2S)	4961(52)	4447(61)	−703(41)	297(57)
C(3S)	5212(22)	5095(60)	−79(67)	263(43)
P(1)	9614(4)	1014(6)	2880(4)	49(2)
C(111)	10204(14)	419(17)	3639(20)	56(10)
C(112)	10396(16)	642(24)	4378(17)	76(12)
C(113)	10819(15)	129(30)	4973(20)	72(12)
C(114)	11035(19)	−604(32)	4761(26)	96(15)
C(115)	10854(20)	−896(26)	4051(27)	107(15)
C(116)	10413(16)	−382(24)	3463(20)	77(11)
C(121)	9614(15)	2104(19)	3239(18)	55(9)
C(122)	9151(14)	2366(24)	3548(17)	72(11)
C(123)	9166(18)	3221(26)	3827(21)	92(14)
C(124)	9652(23)	3745(24)	3832(19)	86(12)
C(125)	10093(16)	3489(24)	3508(20)	72(11)
C(126)	10100(18)	2645(25)	3236(16)	72(11)
C(131)	10030(16)	1121(22)	2168(15)	61(9)
C(132)	9633(15)	1311(26)	1440(19)	102(15)
C(133)	9947(23)	1518(32)	902(22)	141(20)
C(134)	10628(19)	1394(25)	1114(24)	104(15)
C(135)	11013(17)	1196(23)	1796(23)	85(12)
C(136)	10707(19)	1085(23)	2352(17)	74(11)
P(2)	6798(4)	2312(5)	2364(5)	48(2)
C(211)	5885(15)	2262(22)	2015(14)	50(9)
C(212)	5504(18)	2962(24)	1762(16)	82(12)
C(213)	4789(20)	2919(30)	1498(18)	96(14)
C(214)	4476(18)	2208(27)	1519(21)	82(13)
C(215)	4861(19)	1478(24)	1744(21)	89(12)
C(216)	5543(15)	1513(23)	1992(17)	69(10)
C(221)	6989(15)	2761(22)	3307(20)	64(10)
C(222)	6734(15)	3507(22)	3460(20)	65(9)
C(223)	6901(18)	3836(22)	4168(22)	68(10)
C(224)	7349(20)	3470(24)	4752(23)	88(13)
C(225)	7602(17)	2655(27)	4669(19)	90(12)
C(226)	7423(17)	2340(18)	3910(20)	67(10)
C(231)	7009(15)	3162(20)	1809(21)	67(11)
C(232)	7512(20)	3700(23)	2167(23)	91(13)
C(233)	7769(29)	4404(35)	1736(40)	186(35)
C(234)	7419(36)	4307(36)	1070(46)	229(52)
C(235)	6945(31)	3817(37)	592(23)	198(33)
C(236)	6682(17)	3266(29)	1030(18)	117(17)
P(3)	6951(4)	−2031(5)	1624(4)	40(2)
C(311)	6037(12)	−1954(17)	1215(13)	33(7)
C(312)	5669(17)	−2126(21)	1684(18)	69(10)
C(313)	4940(19)	−2040(23)	1346(21)	79(12)
C(314)	4666(20)	−1736(30)	614(24)	118(16)
C(315)	5066(15)	−1596(22)	198(17)	70(11)
C(316)	5734(14)	−1662(21)	507(15)	58(9)
C(321)	7195(17)	−2699(20)	934(16)	53(9)
C(322)	7878(17)	−2741(17)	1038(15)	54(9)
C(323)	8110(14)	3277(19)	576(17)	63(10)
C(324)	7652(17)	−3639(19)	−26(15)	54(9)
C(325)	6999(15)	−3651(18)	−127(14)	42(8)
C(326)	6747(16)	−3145(21)	329(18)	67(10)
C(331)	7104(14)	−2805(19)	2404(14)	40(8)
C(332)	6935(18)	−3648(19)	2253(19)	66(11)
C(333)	7007(17)	−4226(21)	2814(20)	75(11)
C(334)	7268(17)	−3982(19)	3564(18)	67(10)
C(335)	7447(14)	−3171(19)	3738(16)	50(8)
C(336)	7356(12)	−2578(17)	3131(17)	45(8)

[a] Defined as 1/3 of the trace of normalized U_{ij} tensor.

low, $Os_2(CO)_4(\mu\text{-}I)_2(PPh_3)_2$ (**4**) (21 mg, 19.7%); red, $Pt_2Os(CO)_3(\mu\text{-}I)_2(PPh_3)_3$ (**3**) (21 mg, 14.75%). For $Os_2(CO)_4(\mu\text{-}I)_2(PPh_3)_2$ (**4**); IR spectrum (ν_{CO}, cm^{-1}, CCl_4): 2022s, 1987m, 1952s. Mass spectrum displays the parent ion with m/z 1274 (^{192}Os).

3.4. Synthesis of ^{187}Os-labeled complexes 2′, 3′ and 4′

The synthesis of **2′**, **3′** and **4′** was performed analogously to **2**, **3** and **4** using $^{187}Os_2(CO)_6(\mu\text{-}I)_2$ and $Pt(PPh_3)_2(PhCCPh)$ as starting compounds. R_f values and IR spectra of obtained complexes correspond to those previously obtained.

3.5. Structure determination

The structures of $Os_2(CO)_5(\mu\text{-}I)_2(PPh_3)$ and $Pt_2Os(CO)_3(\mu\text{-}I)_2(PPh_3)_3$ were proved by single crystal X-ray structural analysis of the single crystals of **2** and $\mathbf{3} \cdot \frac{1}{2}C_6H_{14}$ obtained from hexane:CH_2Cl_2 and hexane:ether mixtures respectively (Table 3). Stability of the crystals during diffraction experiments was controlled by measuring three check reflections. Their intensities showed no significant variations. Absorption corrections were taken using information on crystal size and shape for **3** and the DIFABS program [36] for **2**. At the absorption correction all unobserved reflections were excluded from the subsequent calculations. Structures were solved by direct methods using the SHELXS-86 program [37] and refilled by full-matrix least squares

Table 6
Bond distances for **2**

Atoms	Bond length (Å)	Atoms	Bond length (Å)
Os(1)–Os(2)	2.717(3)	Os(2)–C(21)	1.81(4)
Os(1)–I(1)	2.765(3)	Os(2)–C(22)	1.78(3)
Os(1)–I(2)	2.760(3)	Os(2)–O(23)	1.84(4)
Os(1)–P(1)	2.379(9)	C(11)–O(11)	1.20(3)
Os(1)–O(11)	1.82(3)	C(12)–O(12)	1.24(4)
Os(1)–C(12)	1.72(3)	C(21)–O(21)	1.19(4)
Os(2)–I(1)	2.730(3)	C(22)–O(22)	1.21(4)
Os(2)–I(2)	2.733(3)	C(23)–O(23)	1.24(4)

method using the SHELXL-93 program [38] using observed reflections only.

In **3** all non-hydrogen atoms were refined anisotropically using independent observed reflections. Os and Pt atoms were distinguished taking into account their ligand environment. Some phenyl rings and solvent molecule undergo high thermal motions. Our attempts to resolve possible disorder were unsuccessful. The structure of **2** was refined in anisotropic approximation for the Os, I and P and isotropic for the remaining atoms using all independent reflections. We were unable to refine anisotropic thermal parameters for C and O atoms in **2** due to the high absorption effect. Hydrogen atoms in both cases were refined in rigid body approximation. Atomic coordinates are given in Tables 4 and 5, and selected bond lengths are in Tables 2 and 6. Tables of thermal parameters, hydrogen atom coordinates and full lists of bond distances and angles have been deposited at the Cambridge Crystallographic Data Centre.

It should be mentioned that diffraction data for **2** given in Table 3 were measured from the orange hexagonal-plate single crystal. But the crystallization product also contained a small portion of yellow long needle-like plates. For one of them with size of $0.05 \times 0.12 \times 0.25\,mm^3$ a full set of diffraction data were measured. The cell parameters, atomic coordinates and geometrical characteristics calculated were found to be close to those for **2** within $\pm 3\sigma$ range. The difference in color may be probably conditioned by dichroism or imperfection of the crystals.

References

[1] R.D. Adams, in D.F. Shriver, H.D. Kaesz and R.D. Adams (eds.), *The Chemistry of Metal Cluster Complexes*, VCH, New York, 1990, p. 130.

[2] (a) V.A. Maksakov, V.P. Kirin, A.V. Virovets, N.V. Podbereskaya and P.P. Semyannikov, *J. Organomet. Chem.*, in press. (b) A.V. Virovets, N.V. Podbereskaya, V.A. Maksakov and V.P. Kirin, *Abstr. Pap. XII European Crystallography Meet., Moscow, 1982*, p. 332.

[3] D.A. Roberts and G.L. Geoffroy, in G.W. Wilkinson, F.G.A. Stone and E.W. Abel (eds.), *Comprehensive Organometallic Chemistry*, Vol. 6, Elsevier, New York, 1982, p. 763.

[4] E.E. Sutton, M.L. Niven and J.R. Moss, *Inorg. Chim. Acta, 70* (1983) 207.

[5] M.I. Bruce, M.R. Show and E.R.T. Tieking, *Austr. J. Chem., 39* (1986) 2145.

[6] M.I. Bruce, J.G. Matisons, B.W. Skelton and A.H. White, *Austr. J. Chem., 35* (1982) 687.

[7] A. Madions and P. Woodward, *J. Chem. Soc. Dalton Trans.*, (1975) 1534.

[8] L.J. Farrugia, J.A.K. Howard, P. Mitrprachon, F.G.A. Stone and P. Woodward, *J. Chem. Soc. Dalton Trans.*, (1981) 162.

[9] S.P. Gubin, *Khimiya Klasterov*, Nauka, Moscow, 1987, p. 263.

[10] J.P. Collman, L.S. Heddegus, J.R. Norton and R.G. Finke, *Principles and Applications of Organotransition Metal Chemistry*, University Science Books, Mill Valley, CA, 1987.

[11] S.S. Batsanov, *Zh. Neorganich. Khim., 36* (1991) 3015.

[12] M.M. Grutchfield, C.H. Dungan, J.H. Letcher and J.R. Van Waser, *^{31}P Nuclear Magnetic Resonance, Topic in Phosphorus Chemistry*, Vol. 5, Interscience New York, 1967.

[13] J. Mason, *Multinuclear NMR*, Plenum, New York, 1987, p. 73.

[14] P.S. Pregosin and R.W. Kung, *NMR Basic Principles and Progress*, Vol. 16, Springer, Heidelberg, 1979.

[15] J.W. Emsley, J. Feeney and L.H. Sutcliff, *High Resolution Nuclear Magnetic Resonance Spectroscopy*, Pergamon, Oxford, 1965.

[16] Y. Koie, S. Shinoda and Y. Saito, *Inorg. Chem., 20* (1981) 4408.

[17] G.W. Bushnell, D.T. Eadic, A. Pidcock, A R. Sam, R.D. Holines-Smith, S.R. Stobart, E.T. Brennan and T.S. Cameron, *J. Am. Chem. Soc., 104* (1982) 5837.

[18] L.J. Farrugia, J.A.K. Howard, P. Mitrprachon, F.G.A. Stone and P. Woodward, *J. Chem. Soc. Dalton Trans.*, (1981) 155.

[19] P.L. Bellon, A. Ceriotti, F. Demortin, G. Longoni and B.T. Heaton, *J. Chem. Soc. Dalton Trans.*, (1982) 1671.

[20] P. Braunstein, E. de Jesus, A. Dedieu, M. Lanfranchi and A. Tiripicchio, *Inorg. Chem., 31* (1992) 399.

[21] Y. Koie, S. Shinoda and Y. Saito, *J. Chem. Soc. Dalton Trans.*, (1981) 1082.

[22] A. Moor, R.S. Pregosin and L.M. Venanizi, *Inorg. Chim. Acta, 61* (1982) 135.

[23] B.F.G. Johnson and A. Rodgers, in D.F. Shriver, H.D. Kaesz and R.D. Adams (eds.), *The Chemistry of Metal Cluster Complexes*, VCH, New York, 1990, p. 303.

[24] B.W. Clare, M.C. Favas, D.L. Kepert and A.S. May, *Adv. Dynamic Stereochem., 1* (1985) 1.

[25] G.G. Mathur, A. Pidcock and G.J.N. Rapsey, *J. Chem. Soc. Dalton Trans.*, (1973) 2095.

[26] R.J. Blau and J.H. Espenson, *Inorg. Chem., 25* (1986) 878.

[27] A. Moor, R.S. Pregosin and L.M. Venanzi, *Inorg. Chim. Acta, 48* (1981) 153.

[28] J.C. Jeffery, H. Easay and F.G.A. Stone, *J. Chem. Soc. Dalton Trans.*, (1982) 1733.

[29] M.J. Chetcuti, K. Marsden, I. Moore, F.G. Stone and P. Woodward, *J. Chem. Soc. Dalton Trans.*, (1982) 1749.

[30] M.J. Chetcuti, J.A.K. Howard, R.M. Mills, F.G. Stone and P. Woodward, *J. Chem. Soc. Dalton Trans.*, (1982) 1757.

[31] T.V. Asworth, J.A.K. Howard and F.G.A. Stone, *J. Chem. Soc. Dalton Trans.*, (1980) 1609.

[32] T.V. Asworth, M. Berry, J.A.K. Howard, M. Lugano and F.G.A Stone, *J. Chem. Soc. Dalton Trans.*, (1980) 1615.

[33] M.I. Bruce, M. Cooke, M. Greene and D.J. Westlake, *J. Chem. Soc.*, (1968) 987.

[34] K. Moseley and P.M. Maitlis, *J. Chem. Soc. Dalton Trans.*, (1974) 169.

[35] D.M. Blake and D.M. Rounhill, *Inorg. Synth., 18* (1978) 122.

[36] N. Walker and D. Stuart, *Acta Crystallogr. Sect. A:, 39* (1983) 158.

[37] G.M. Sheldrick, *Acta Crystallogr. Sect. A:, 46* (1990) 467.

[38] G.M. Sheldrick, *Acta Crystallogr. Sect. A:, 49* (1993) C53.